



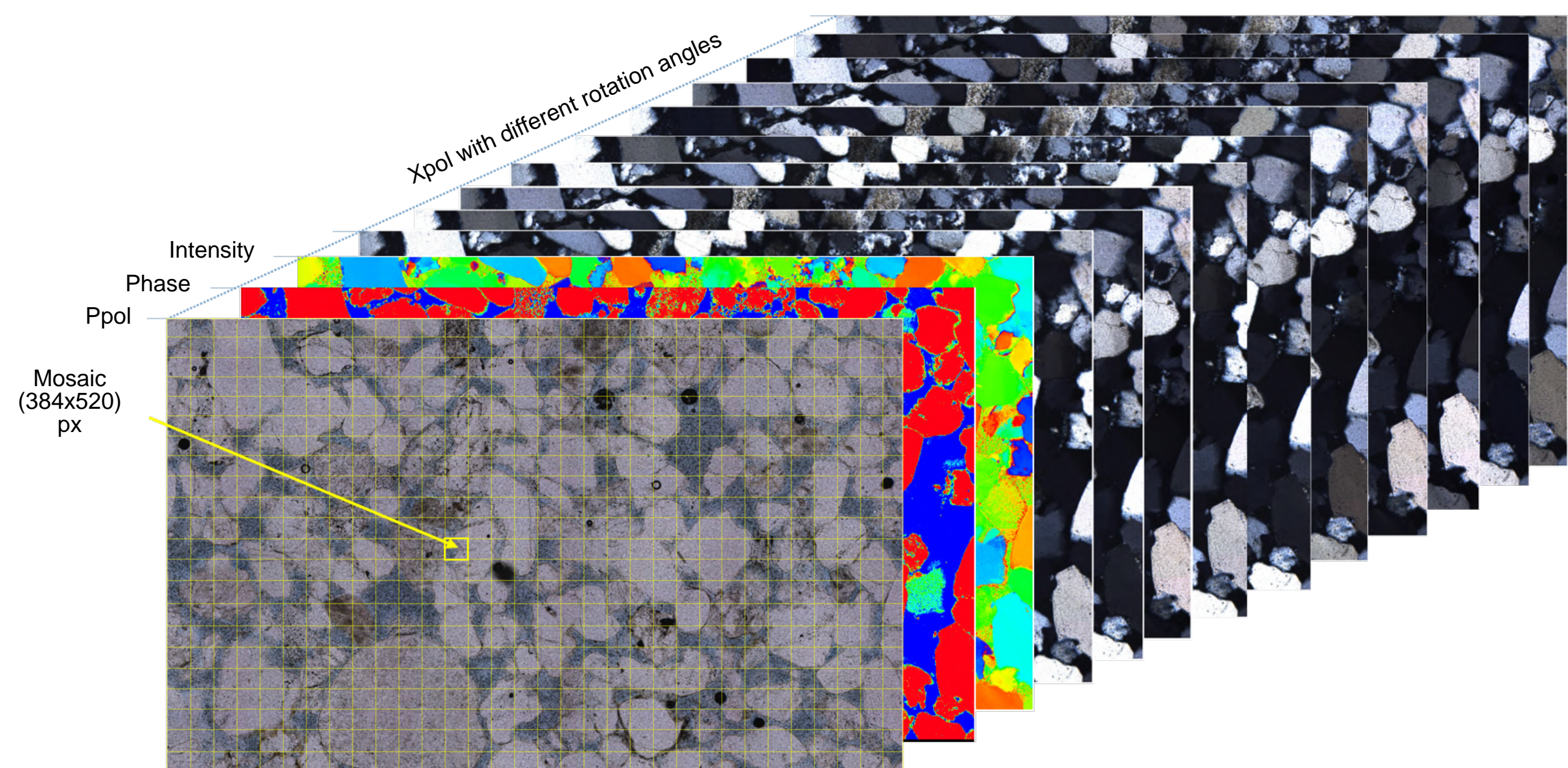
Motivation

Mineral thin sections contain a treasure of information. It is anticipated that thin section samples can be systematically and quantitatively analyzed with a specifically designed system equipped with ML approaches or deep learning methods such as CNNs. However, all of previous studies related to automatic petrographic analysis are restricted by the insufficiency of the training data. As strengthened by the paucity of large volume of well-labeled data significantly impeded the development of novel deep learning methods. In this context, the main motivation of this thesis is to close this data gap by building a consistent and sufficiently large training dataset that can be used to develop advanced ML- and DL-based applications for petrographic identification.



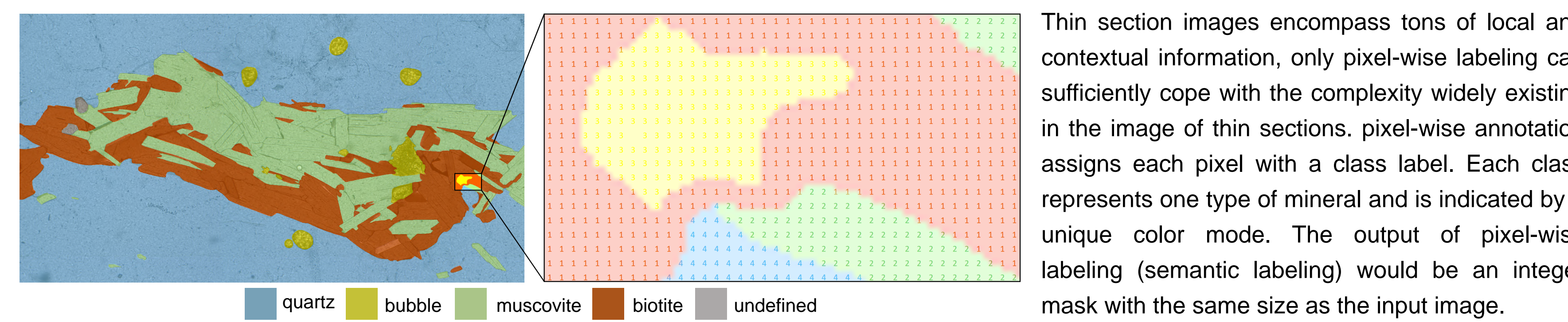
Fig. 1. Timeline of ML and deep learning-based approaches for petrographic analysis. The drawbacks existing in the research are marked with different color-coded dots. ● small training dataset, ● insufficient data, ● closed dataset, ● low generalization capacity, ● feature engineering, ● images are taken under static lighting and polarisations, ● information loss in the dataset.

ViP Data Set



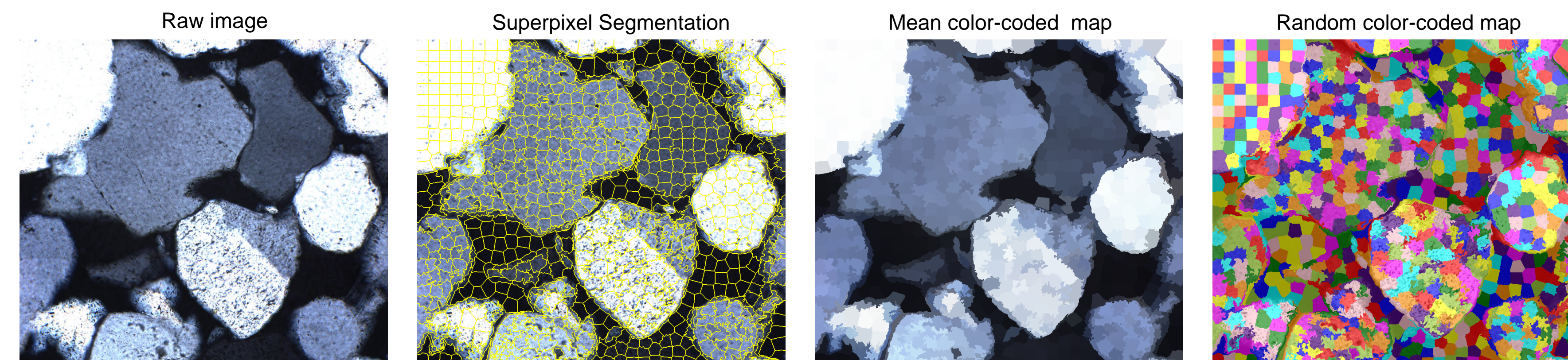
The raw data set is generated by virtual petrographic microscopy (ViP), a cutting-edge methodology that can automatically scan entire thin section in gigapixel resolution. The scanning process is performed sequentially along a predefined grid and repeated for different rotation angles of crossed polarizers. The scanned mosaic image can be precisely overlapped which allows to interpolate and to fit the extinction behavior of each individual pixel as a smooth function. Based on the interpolated extinction information, a phase map qualitatively showing the mineral axis misorientations can be produced. Extra complementary image layers reflecting chemical and physical information of the thin section can be stacked along the third axis to the image cube.

Image Annotation



Thin section images encompass tons of local and contextual information, only pixel-wise labeling can sufficiently cope with the complexity widely existing in the image of thin sections. pixel-wise annotation assigns each pixel with a class label. Each class represents one type of mineral and is indicated by a unique color mode. The output of pixel-wise labeling (semantic labeling) would be an integer mask with the same size as the input image.

Image annotation, especially pixel-wise annotation is always time-consuming and inefficient. Moreover, it would be particularly challenging when to manually create dense semantic labels for ViP data in view of its size and dimensionality. To address this problem, we proposed a human-computer collaborative annotation pipeline where computers extract image boundaries by splitting images into superpixels, while human-annotators subsequently associate each superpixel manually with a class label with a single mouse click or brush stroke. This frees the human annotator from the burden of painstakingly delineating the exact boundaries of grains and it has the potential to significantly speed up the annotation process.



Pixels are rectangular basic units of images, whereas Superpixels (SPs) are a group of pixels that are perceptually similar. Instead of providing a discrete representation of images, superpixels are better aligned with image edges and largely reduce the image complexity. Unlike object segmentation that aims to find hard decisions about the outline of the object, superpixels generate a controlled oversegmentation of images from which the shape of grains can be recovered in the subsequent processing. Usually, if K represents the number of objects in the image, $P = m \times n$ is the number of pixels of the input image where m , n is the height and width [px] of the given image, then for the number of superpixels N :

$$K \ll N \ll P$$

Superpixel Benchmarks

Given an image I having N pixels, $S = \{S_1, \dots, S_m\}$ is superpixel segmentation, $G = \{G_1, \dots, G_n\}$ is ground truth segmentation, metrics are defined as:

- **Boundary Recall** assessed how well the superpixel boundaries aligned with the ground-truth edges

$$Rec(G, S) = \frac{TP(G, S)}{TP(G, S) + FN(G, S)}$$

- **Compactness** measures the similarity of a single superpixel to a circle

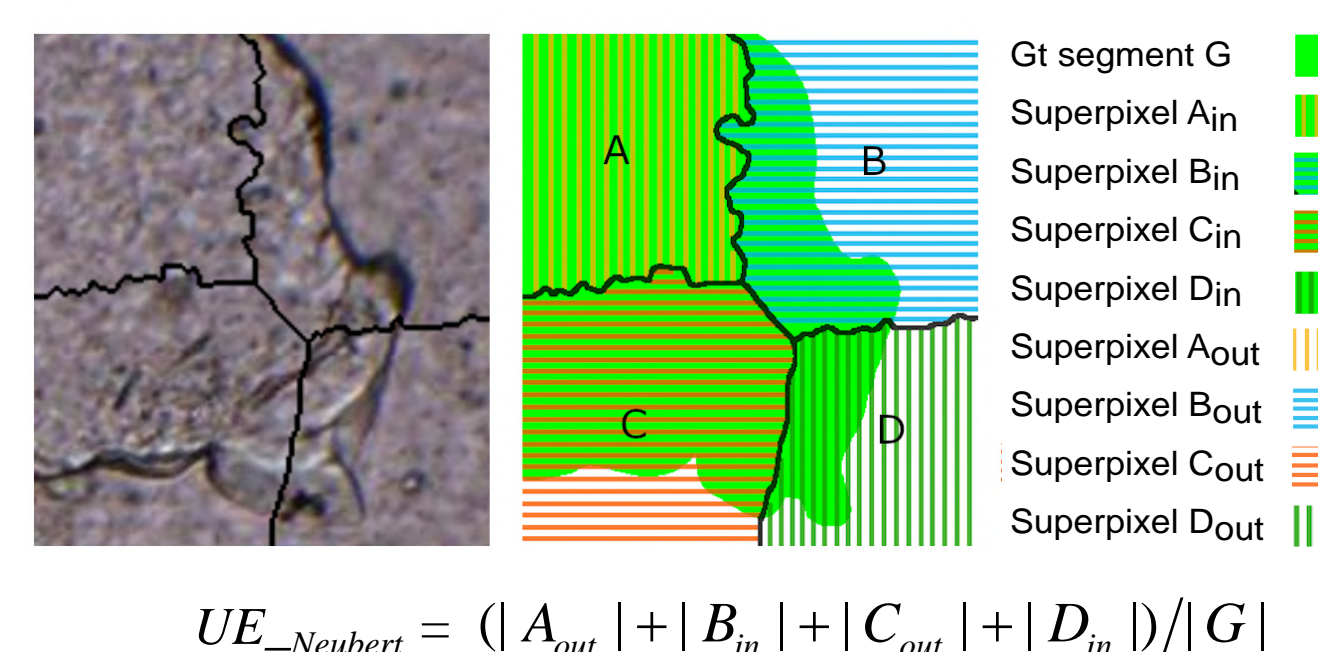
$$CO(G, S) = \frac{1}{N} \sum_{S_j} |S_j| \frac{4\pi A(S_j)}{P(S_j)}$$

- **Explained Variation** provides a human-independent quantification

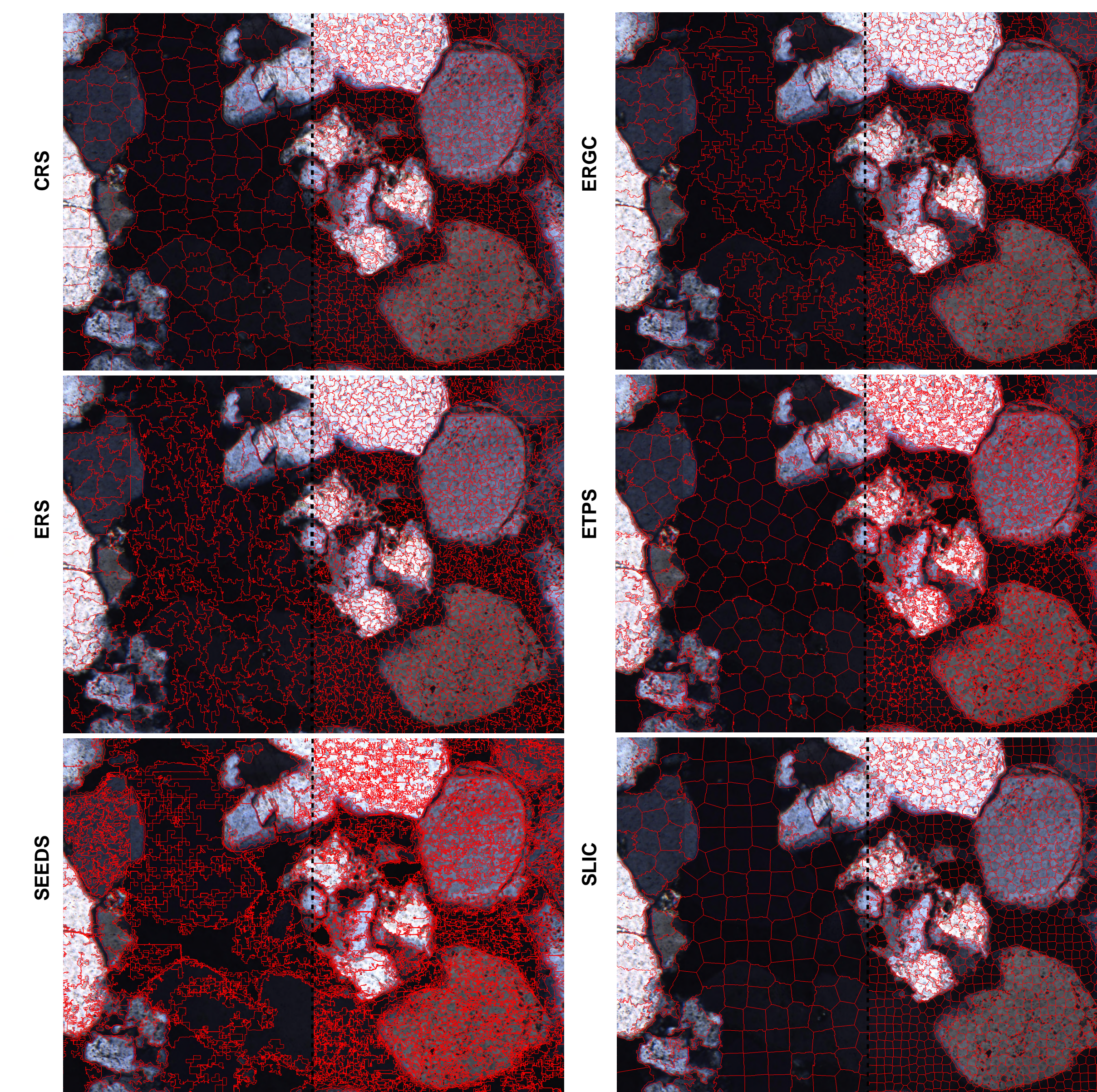
$$EV(S) = \frac{\sum_{S_j} |S_j| (\mu(S_j) - \mu(I))^2}{\sum_{x_n} (I(x_n) - \mu(I))^2}$$

- **Undersegmentation Error** measures the total amount of superpixel leak with respect to the ground-truth segment border

$$UE(G, S) = \frac{1}{N} \sum_{G_i} \sum_{S_j | G_i \neq S_j} \min\{|S_j \cap G_i|, |S_j - G_i|\}$$



Superpixel Evaluation



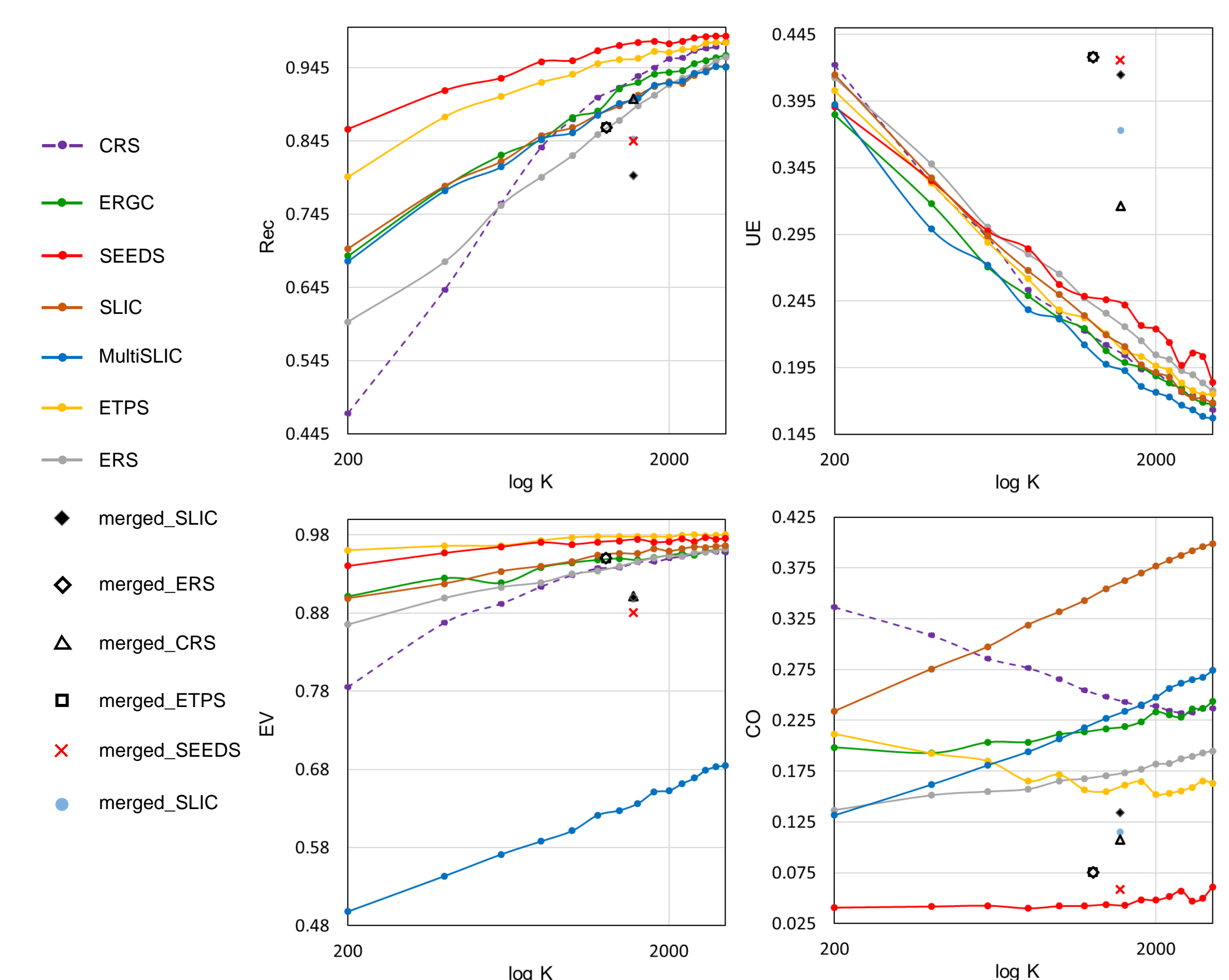
Motivated by the restriction to the input dimensionality of the existing algorithms, a novel adaption for established SLIC is proposed: MultiSLIC which can take in multiple information layers to extract superpixels

Single image plane Multiple image planes

Superpixel Merging



The performances of tested algorithms are compared with respect to Rec , UE , EV and CO . Ideal approach to be used in the annotation pipeline should have excellent boundary adherence with low boundary leakage, therefore, Rec and UE are given prior attention. The existing results demonstrate that ETPS and SEEDS are considerably better performing than others in many aspects. ETPS also makes a good trade-off between the compactness of superpixels and boundary adherence. Although MultiSLIC shows advantages in detecting the region boundaries for small K , it cannot compete with SEEDS and ETPS for $K=3000$. On the other hand, merged superpixel segmentation provides less redundant representation for original images than initial superpixel segmentation, but quantitatively, the boundary recall of merged segmentation is largely reduced compared to the one that is not merged.



References

Baykan, N. A., & Yilmaz, N. (2010). Mineral identification using color spaces and artificial neural networks. *Computers & Geosciences*, 36(1), 91-97.

Borges, H. P., & de Aguiar, M. S. (2019). Mineral Classification Using Machine Learning and Images of Microscopic Rock Thin Section. In *Mexican International Conference on Artificial Intelligence*, pp. 63-76.

Budennyy, S., Pachezhertsev, A., Bukharev, A., Erofeev, A., Mitrushkin, D., & Belozorov, B. (2017). Image processing and machine learning approaches for petrographic thin section analysis. In *SPE Russian Petroleum Technology Conference*.

Cheng, G., & Guo, W. (2017). Rock images classification by using deep convolution neural network. In *Journal of Physics: Conference Series*, Vol. 887(1), p. 012089.

Iglesias, J. C. A., Santos, R. B. M., & Paciomnik, S. (2019). Deep learning discrimination of quartz and resin in optical microscopy images of minerals. *Minerals Engineering*, 138, 79-85.

Jiang, F., Gu, Q., Hau, H., & Li, N. (2017). Grain segmentation of multi-angle petrographic thin section microscopic images. In *2017 IEEE International Conference on Image Processing (ICIP)*, pp. 3879-3883.

Karimpouli, S., & Tahmasebi, P. (2019). Segmentation of digital rock images using deep convolutional autoencoder networks. *Computers & Geosciences*, 126, 142-150.

Li, N., Hao, H., Gu, Q., Wang, D., & Hu, X. (2017). A transfer learning method for automatic identification of sandstone microscopic images. *Computers & Geosciences*, 103, 111-121.

Marmo, R., Amodio, S., Tagliaferrari, R., Ferreri, V., & Longo, G. (2005). Textural identification of carbonate rocks by image processing and neural network: Methodology proposal and examples. *Computers & Geosciences*, 31(5), 649-659.

Mlynarczuk, M., Górszczyk, A., & Šlapek, B. (2013). The application of pattern recognition in the automatic classification of microscopic rock images. *Computers & Geosciences*, 60, 126-133.

Ramil, A., López, A., Pozo-António, J., & Rivas, T. (2018). A computer vision system for identification of granite-forming minerals based on RGB data and artificial neural networks. *Measurement*, 117, 90-95.

Singh, N., Singh, T., Tiwary, A., & Sarkar, K. M. (2010). Textural identification of basaltic rock mass using image processing and neural network. *Computational Geosciences*, 14(2), 301-310.

Šlapek, B., & Mlynarczuk, M. (2013). Application of pattern recognition methods to automatic identification of microscopic images of rocks registered under different polarization and lighting conditions. *Geology, Geophysics Environment*, 39(4), 373.

Tang, D., & Spikes, K. (2017). Segmentation of shale SEM images using machine learning. In *SEG Technical Program Expanded Abstracts 2017* (pp. 3898-3902). Society of Exploration Geophysicists.

Thompson, S., Fueten, F., & Bockus, D. (2001). Mineral identification using artificial neural networks and the rotating polarizer stage. *Computers & Geosciences*, 27(9), 1081-1089.

Zhang, Y., Li, M., Han, S., Ren, Q., & Shi, J. (2019). Intelligent Identification for Rock-Mineral Microscopic Images Using Ensemble Machine Learning Algorithms. *Sensors*, 19(18), 3914.